Femtosecond laser-induced nanofabrication in the near-field of atomic force microscope tip

A. Kirsanov, A. Kiselev, and A. Stepanov[a)]
Institute of Applied Physics of Russian Academy of Science, 603950, 46 Ulianov Street, Nizhny Novgorod, Russia

N. Polushkin
Institute for Physics of Microstructures of Russian Academy of Science, 603600, Nizhny Novgorod, GSP-105, Russia

(Received 13 May 2003; accepted 3 September 2003)

The formation of nanocraters on the surface of metallic films under the tip of an atomic force microscope by femtosecond laser pulses is demonstrated. The influence of laser polarization, pulse duration, and tip–sample distance on threshold fluence for nanoprocessing is investigated. Analysis of experiments shows that heating of the tip by laser radiation and its lengthening is the predominant mechanism for laser-induced nanoprocessing. © *2003 American Institute of Physics.*
[DOI: 10.1063/1.1621722]

I. INTRODUCTION

The formation of nanostructures on the surface of different materials is a field of research activity that has attracted much attention in recent years. One of the methods to produce nanostructures is to illuminate the gap between the tip of an atomic force microscope (AFM) or scanning tunneling microscope and a substrate surface by laser radiation. In such a way, hillocks and pits with a diameter up to 20–30 nm on the surface from different materials have been created.[1–3] Two mechanisms explaining the observed nanostructuring are discussed in the literature. One mechanism is the substrate material ablation by a laser electric field enhanced in the vicinity of the tip apex.[1,4] The other is mechanical stress by the heated tip as a result of thermal expansion of the tip due to absorption of laser radiation.[3,5,6] Despite the large effort made to clarify the problem, there is still controversy over the explanation of nanoproccessing. In this article, we present results of several experiments performed with laser pulses of femtosecond duration in order to contribute further to the discussions on nanostructuring mechanisms. The use of ultrashort laser pulses introduces a parameter (pulse duration), which is important for better understanding of the problem. In addition, the femtosecond duration of laser pulses enlarges the range of materials that can be developed.

II. EXPERIMENTAL SETUP AND RESULTS

A simplified experimental setup is depicted in Fig. 1. The radiation from a femtosecond laser ($\lambda=0.8\ \mu$m, $\tau=100$ fs, $W\leqslant 50\ \mu$J) is focused by a lens to a focal spot 300 μm in diameter in a tip–surface gap. The angle of incidence is $\Theta=17°$ relative to the substrate surface. The polarization of the laser radiation was varied during the experiments. A commercial AFM system (Smena model from NT-MDT) was employed. Silicon tips covered by a 20–30 nm layer of W_2C with a radius of curvature $r\approx 30$ nm were used. The samples are metallic films (In, Au, Cu, magnetic material FeCr) with a thickness of 20–30 nm on a Si substrate. The films are deposited by the sputtering technique. The scanning probe microscope is used mainly in contact mode.

When the fluence is above a certain threshold value, processing of craters on the film surface occurs. Figure 2 shows a crater on an FeCr film produced by a pulse with fluence $F=95\ \text{mJ/cm}^2$. The image was taken by the AFM immediately after processing. The craters are, typically, 30–50 nm in diameter and 3–10 nm in height, similar to the results of Jersch[1] and Lu[7]. The threshold fluence depends on the material of the film. In Fig. 3, the dependence of the threshold fluence on the melting temperature for different materials of sample films is presented. The dependence is approximately linear. It was observed that the threshold fluence F_{th} is influenced by the polarization of the laser radiation. When p polarization with respect to the substrate surface is used, the value of the threshold fluence is 1.5–2 times lower than for perpendicular s polarization. Thus, for FeCr $F^p_{\text{th}}=75\pm 10\ \text{mJ/cm}^2$, $F^s_{\text{th}}=150\pm 15\ \text{mJ/cm}^2$, and for Au $F^p_{\text{th}}=34\pm 5\ \text{mJ/cm}^2$, $F^s_{\text{th}}=67\pm 10\ \text{mJ/cm}^2$.

The threshold fluence for femtosecond and nanosecond laser pulses was compared. To produce nanosecond pulses, a

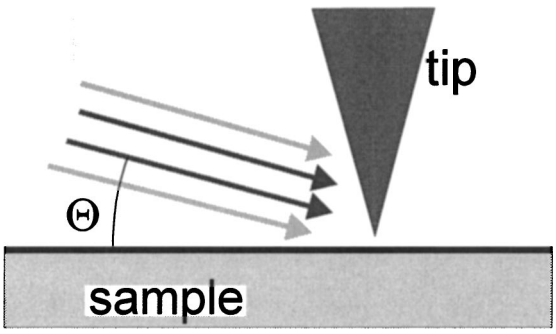

FIG. 1. Diagram of the experimental setup.

[a)]Electronic mail: step@ufp.appl.sci-nnov.ru

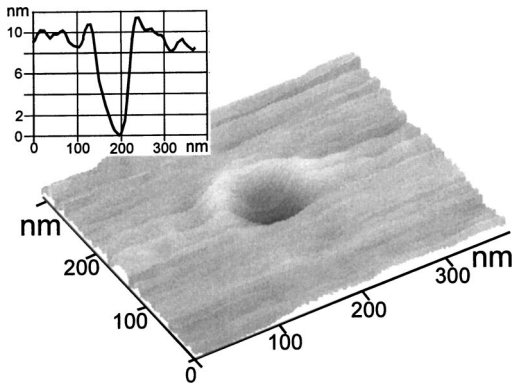

FIG. 2. AFM image of a crater made with W_2C-coated silicon tip on a FeCr film, p polarization, and $F=95\ \mathrm{mJ/cm^2}$.

regenerative amplifier of the laser system was used in the regime of lasing (without femtosecond pulse injection). The pulse duration in this case was $\tau_{ns}\approx 9$ ns. Threshold fluences $F_{th}^{p}=46\pm 5\ \mathrm{mJ/cm^2}$ and $F_{th}^{s}=115\pm 10\ \mathrm{mJ/cm^2}$ for nanofabrication on a gold film were measured with nanosecond pulse duration (as compared to $F_{th}^{p}=34\pm 5\ \mathrm{mJ/cm^2}$ and $F_{th}^{s}=67\pm 10\ \mathrm{mJ/cm^2}$ for femtosecond pulses). For In film, $F_{th}^{p}=7\pm 2\ \mathrm{mJ/cm^2}$ (femtosecond pulses) and $F_{th}^{p}=20\pm 3\ \mathrm{mJ/cm^2}$ (nanosecond pulses) were measured. Thus, for nanosecond pulse duration the threshold fluences exceed the case with femtosecond pulses by ~1.5–2.5 times.

The dependence of the threshold fluence for a FeCr film on a distance between the tip and the sample surface for the p polarization is depicted in Fig. 4. There is no dependence within the experimental error.

III. DISCUSSION OF EXPERIMENTAL RESULTS

Let us now discuss our experimental results from the point of view of the two mechanisms of nanoprocessing that have been considered in the Introduction. A quantitative description of the field enhancement in the vicinity of the tip apex requires a complex calculation procedure, which was performed in certain approximations in the literature.[7,8] Numerical calculations of thermal lengthening of the tip in an axially symmetric field were made in Ref. 9, and in a plane wave in Ref. 6. However, it is advantageous to write down a simple analytical model of the thermal lengthening of the tip, which will be more convenient for subsequent analysis. In this respect, some estimations have been made in the literature.[3,5] Below, we will develop a model that will include the main parameters of the materials of the tip and samples, as well as the characteristics of the laser field, which are essential for analysis of experiments.

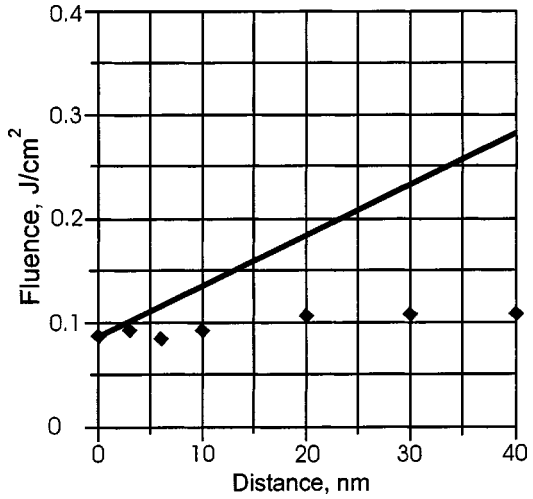

FIG. 4. Threshold fluence vs tip–sample distance.

A. Model of thermal lengthening of the tip

First, we will find absorption of laser radiation by a conical tip of the atomic force microscope. Using the Fresnel formulas[10] we find the dependence averaged over the conical surface intensity reflectivity $A(\delta)$ for tungsten on polarization (Fig. 5). The values of optical constants appearing in the Fresnel formulas ($n=3.7$, $k=2.7$) are taken from Ref. 11. The dependence shows that the absorption for p ($\delta=0°$) and s ($\delta=90°$) polarizations differs by no more than 20%.

To estimate heating of the AFM tip we assume that the conical slice with thickness dz (Fig. 6) absorbs the energy of

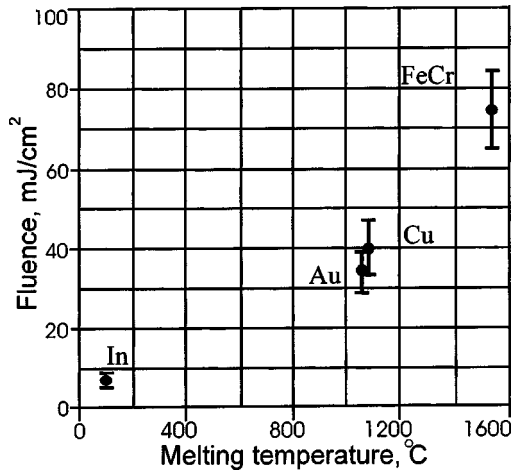

FIG. 3. Threshold fluence vs melting temperature for different materials.

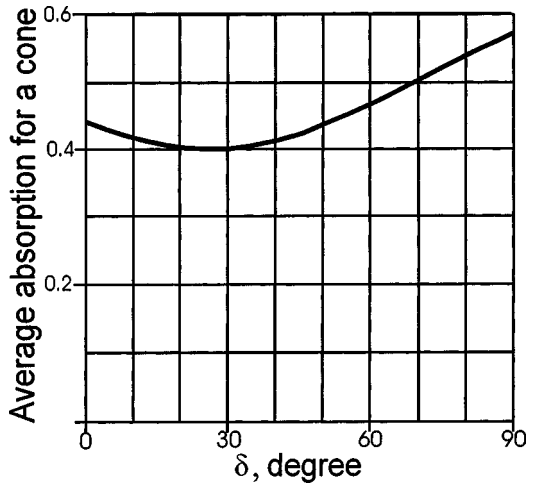

FIG. 5. Absorption averaged over conical surface as a function of polarization.

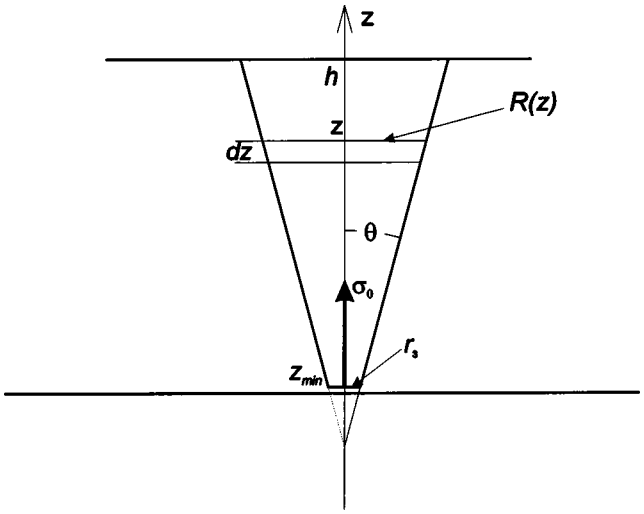

FIG. 6. Geometry underlying the model of a tip.

incident radiation according to the calculated absorption coefficient, and that this energy heats the conical slice. In other words, we neglect the heat flow along the tip axis, which is justified for actual tips with relatively small vertex angles at times $\leqslant 10$ ns (see, e.g., Ref. 6). Then, for the temperature along the tip axis we will have:

$$T(z)=\frac{FA(\delta)dS}{c\rho dV},$$

where F is the incident fluence, $A(\delta)$ is the absorption coefficient, c and ρ are the specific heat capacity and density for tip material, and dS and dV are the effective area and volume of the conical slice with thickness dz. Substituting expressions for dS and dV yields the following expression for the temperature dependence along the tip:

$$T(z)=\frac{2FA(\delta)}{\pi c\rho z tg\,\theta}, \tag{1}$$

i.e., with decreasing z, the temperature increases and the maximum temperature will be at the very tip apex. The minimum value of $z_{\min}$ at which the formula (1) still works is determined by applicability of Fresnel formulas and is fractions of wavelengths of incident radiation.

Heating leads to tip lengthening, each conical layer with thickness dz being enlarged by $dl=\alpha T(z)dz$, where α is the coefficient of thermal expansion of the tip material. Integrating with respect to z yields the total lengthening of the tip:

$$L_{\text{therm}}=\int_{z_{\min}}^{h}\alpha T(z)dz=\frac{2\alpha FA(\delta)\ln(h/z_{\min})}{\pi c\rho tg\,\theta}. \tag{2}$$

In Eq. (2) h is the length of the tip.

Two scenarios of nanostructure formation by tip heating and lengthening can be considered. The first is that the tip apex is heated up to a temperature that exceeds the melting temperature of sample material T_m, then comes in close mechanical contact with the sample due to thermal expansion and melts the sample. In this case, the criterion for nanostructuring is the achievement of maximum temperature at the tip apex that is equal to the melting temperature of the sample. For threshold fluence this will lead to the following expression:

$$F_{\text{th}}^{\text{therm}}=\frac{\pi c\rho z_{\min} tg\,\theta T_m}{2A(\delta)}. \tag{3}$$

The second scenario relies on the following considerations. The thermal lengthening of the tip can be estimated by Eq. (2), and is resisted by an elastic force from the sample. If pressure by the tip on the sample exceeds some critical value, at which elastic deformation of the sample transforms into plastic, then some traces are left on the sample surface—the observed nanostructures.

In this model, the criterion for the nanostructuring threshold may be obtained from the condition of equality of thermal lengthening of the tip with elastic deformation of the conical tip under external force. The elastic deformation of a conical layer with thickness dz (Fig. 6) is given by the Hooke's law $dl_{\text{elast}}=[\sigma(z)/E]dz$, where E is the Young's modulus of the tip material, and $\sigma(z)$ is the tension on element dz for the conical tip. It can be expressed through tension σ_0 at the tip apex with radius r_3 $\sigma(z)=\sigma_0 r_3^2/R(z)^2=\sigma_0 r_3^2/z^2 tg\,\theta^2$. After integration with respect to z and equating elastic deformation to thermal lengthening of the tip, we obtain the following expression for the nanostructuring threshold:

$$F_{\text{th}}^{\text{mech}}=\frac{\pi c\rho r_3\sigma_0}{2A(\delta)\alpha E\ln(h/z_{\min})}, \tag{4}$$

where σ_0 is some critical tension for sample material, starting from which the tip produces irreversible changes on the sample. If there is a gap L between the tip and the sample, the elastic deformation should compensate for the difference $L_{\text{therm}}-L$, and the expression for threshold fluence will depend on the distance L:

$$F_{\text{th}}^{\text{mech}}(L)=\frac{\pi c\rho tg\,\theta}{2A(\delta)\alpha\ln(h/z_{\min})}\left(\frac{\sigma_0 r_3}{Etg\,\theta}+L\right). \tag{5}$$

Let us present numerical estimates for the heating and lengthening of the tip. For silicon, a material from which the tip is made, $\alpha=2.5\times10^{-6}\,\text{K}^{-1}$, $c=0.71\,\text{J/g K}$, $\rho=2.3\,\text{g/cm}^3$, and $E=120\,\text{GPa}$.[12] Since optical constants for W_2C at the working wavelength are unknown, the absorption coefficient is estimated for W, which is justified by the fact that data on electric conductivity of W_2C and W are very close. Estimates of $z_{\min}$ and σ_0 are difficult to perform. Let us assume that $z_{\min}=0.4\,\mu$m, i.e., equal to a half wavelength of laser radiation. Material science gives several parameters characterizing the beginning of nonelastic deformation of material, and these parameters are functions of temperature and deformation rate.[13] In estimations, we will use data on the dynamic limit of elasticity obtained in experiments with shock waves in steel, and assume $\sigma_0\approx 1$ GPa.[14] However, it should be noted that plastic deformation within existing concepts is related to the motion of dislocations and faults with characteristic scales of $\geqslant 1$ μm.[15] In our case, the affected area is several tens of nanometers, so it is likely that plastic deformation within this scale will be governed by other

mechanisms. Then, one should treat the presented estimate of the dynamic limit of elasticity with much caution, taking it as a lower possible limit. Nevertheless, substituting the above values into formulas for temperature and tip lengthening at fluence $F=100\,\mathrm{mJ/cm^2}$ yields the following estimates $T_{\max}\approx 3000\,\mathrm{K}$, $L_{\mathrm{therm}}\approx 20\,\mathrm{nm}$. Thus, this simplified model shows the heating of the tip up to several thousand K, and more importantly, it demonstrates tip lengthening in the order of tens of nanometers, well in accordance with more rigorous calculations.[6]

Now, taking into account the found relations, let us return to the discussion of experimental results from the point of view of mechanisms for nanoprocessing.

B. Polarization dependence of nanostructuring threshold

In the ablation approach, the field enhancement in the vicinity of tip apex is very sensitive to the polarization of laser radiation relative to the tip axis. If *p*-polarization enhancement in intensity just under the apex may reach several hundreds times, *s* polarization in the field enhancement is almost not observed.[8] Therefore, the nanostructuring threshold in this mechanism must strongly increase when *p* polarization is changed to *s* polarization. In the second mechanism being discussed here, the effect of polarization on heating and thermal lengthening of the tip is mainly determined by the dependence of the absorption coefficient on polarization (Fig. 5). The dependence is very weak; therefore, the results of the experiment, where nanostructuring thresholds for *p* polarization were only 1.5–2 times lower than for *s* polarization, speak for a higher probability of the mechanism of heating and thermal lengthening of the tip.

C. Influence of pulse duration

In the two approaches being discussed here, changes in pulse duration affect, in a different degree, the nanostructuring threshold. In the ablation mechanism, optical radiation is absorbed by electrons in a metallic sample just under the tip with a characteristic spatial scale about the tip apex size. During time τ_1 of several picoseconds, absorbed energy transfers from electrons to the lattice.[16] Then, due to electronic heat conductivity, heat propagates to an area with characteristic spatial scale $l\sim\sqrt{\chi\tau}$, where χ is the coefficient of thermal conductivity of the sample material, and τ is the characteristic time. If the laser pulse duration is $\tau\leqslant\tau_1$ (femtosecond pulses), then for estimation of the characteristic scale we can use τ_1. But, if the laser pulse duration is more than τ_1 (nanosecond pulses), then the characteristic spatial scale of the heated area will be determined by laser pulse duration τ. The volume of the heated area in a thin metallic film on the surface of a poorly conducting material is directly proportional to the second power of the spatial scale. Thus, the volume of the heated area for nanosecond pulse durations will exceed that for femtosecond pulses by $(l_{\mathrm{ns}}/l_{\mathrm{fs}})^2=(\tau/\tau_l)\sim 10^3-10^4$ times. In other words, ablation of sample material by nanosecond pulses requires much higher energy than by femtosecond pulses. On the other hand, pulse duration does not appear in the criteria for the nanostructuring threshold related to the heating and lengthening of the tip [formulas (3) and (4)]. When the formulas were derived, however, it was assumed that heat conductivity has too little time to equalize temperature along the tip axis. Estimates, as well as numerical computations,[6] show that this condition is obeyed up to times ~10 ns, i.e., at pulse duration $\tau=9$ ns, used in the experiment, one may expect some decrease in temperature of the tip apex, in comparison with femtosecond pulses, due to heat outflow. This probably accounts for the experimental fact that the nanostructuring threshold is by ~1.5–2.5 times higher for nanosecond pulses than for femtosecond pulses. Thus, our comparative analysis of nanostructuring thresholds for nanosecond and femtosecond pulse durations indicates the thermal–mechanical mechanism of nanostructure formation on the sample surface.

D. Nanostructuring threshold versus tip–sample distance

The field enhanced near the tip apex decays faster than exponentially versus a distance from the tip.[8,17] This should lead to a strong increase in the nanostructuring threshold with increasing distance between the tip and sample. In the model, when nanostructures are formed by the tip's heating beyond the melting temperature of the sample material [Eq. (3)], the threshold does not depend on tip–sample distance. If nanostructures are formed when the pressure of the tip exceeds some limit value [Eq. (4)], a linear dependence of the threshold on distance should be observed. The dependence of the nanostructuring threshold on distance, plotted by this formula, is shown in Fig. 5 (solid line). Because of the uncertainty in the values of some parameters ($z_{\min}$ and σ_0), the line in Fig. 5 was fitted at $L=0$ to the experimental value of the threshold, and the dependence on distance is given for tip parameters and characteristics used in the estimation of temperature and tip lengthening. Comparison of the above discussions with experimental findings shows that the effect of field enhancement cannot account for the observed dependence of nanostructuring threshold on distance. Moreover, the behavior of the threshold that is almost independent of the value of the tip–sample gap speaks for a high probability of melting of the material by the heated tip. Indirectly, this is evidenced by the fact that the formation of craters and hillocks depends on the relation between the melting temperatures of the tip and sample. If the melting temperature of the tip is higher than that of the sample, the tip melts the sample and produces a crater in it. If the melting temperature of the tip is lower, then hillocks are formed on surface of the sample, which is probably due to shaking off the melted material of the tip on the sample during mechanical contact. This behavior was observed for different pairs of tip–sample materials in all experiments we known.[4,7,18]

One more remark should be made concerning the effect of field enhancement near the tip apex on the process of nanostructuring. Of no doubt, field enhancement does occur, and its order of magnitude corresponds to that numerically estimated in the literature.[7,8] However, a more thorough consideration of the structure of the electric field near the sample surface under the tip shows that the main component of the

field is the component that is perpendicular to the surface. This component, according to the boundary conditions, is ϵ times attenuated inside the sample, where ϵ is the dielectric constant of the sample material. In optics $|\epsilon| \approx 20-25$ for metals,[12] i.e., the intensity of the electromagnetic field, which has been enhanced near the tip apex by 100–500 times,[8] is attenuated inside the metallic sample by $|\epsilon|^2 = 400-600$ times. Undoubtedly, one should consider the field enhancement for dielectric samples when studying surface structures, biological molecules on sample surfaces, etc. However, our analysis of experimental results shows that the role of field enhancement is not important for nanomodification of metallic films.

IV. CONCLUSION

In this article, we have reported results of experimental investigations of the formation of nanostructures on the surface of metallic films just under the apex of an atomic force microscope tip irradiated by a femtosecond laser. The formation of craters with diameter 20–30 nm and depth of several nanometers on the sample surface is demonstrated. Nanostructures in these experiments were produced in different materials ranging from soft and low-melting indium to such hard and high-melting magnetic materials as FeCr. The effect of the dependence of the nanostructuring threshold on the polarization of laser radiation, laser pulse duration, and distance between the tip apex and sample surface has been investigated. An analysis of experimental results was made to understand the mechanism responsible for nanostructuring. Based on this analysis, we may conclude that the main cause of nanostructure formation on the sample surface under laser irradiation of the AFM tip is heating of the tip by absorbed laser radiation and mechanical pressure the tip produces because of its thermal lengthening. The analysis of experimental results shows that the sample material is likely to melt during nanomodification. This, however, requires further experimental verification. In summary, we believe that this investigation has made a next step for the creation of elements of super-high-density optical and magnetic memory up to 1 T bit/cm^2.

[1] J. Jersh and K. Dickmann, Appl. Phys. Lett. **68**, 868 (1996).
[2] S. M. Huang, M. H. Hong, Y. F. Lu, B. S. Lukyanchuk, W. D. Song, and T. C. Chong, J. Appl. Phys. **91**, 3268 (2002).
[3] R. Huber, M. Koch, and J. Feldmann, Appl. Phys. Lett. **73**, 3521 (1998).
[4] A. A. Gorbunov and W. Pompe, Phys. Status Solidi A **145**, 333 (1994).
[5] V. A. Ukraintsev and J. T. Yates, Jr., J. Appl. Phys. **80**, 2561 (1996).
[6] V. Gerstner, A. Thon, and W. Pfeiffer, J. Appl. Phys. **87**, 2574 (2000).
[7] Y. F. Lu, B. Hu, Z. H. Mai, W. J. Wang, W. K. Chim, and T. C. Chong, Jpn. J. Appl. Phys., Part 1 **40**, 4395 (2001).
[8] O. Martin and C. Girard, Appl. Phys. Lett. **70**, 705 (1997).
[9] N. M. Miskovsky, S. H. Park, J. He, and P. H. Cutler, J. Vac. Sci. Technol. B **11**, 366 (1993).
[10] D. A. Stretton, *Theory of Electromagnetism* (Gostechizdat, 1948), p. 540.
[11] *Handbook of Optics*, edited by M. Bass (McGraw-Hill, New York, 1995), Vol. 2.
[12] *Hahdbook of Physical Values*, edited by I. S. Grigoriev (Energoatomizdat, Moscow, 1991) (in Russian).
[13] Ya. B. Fridman, *Mechanical Properties of Metals* (Mashinostroenie, Moscow, 1974) (in Russian).
[14] G. I. Kanel, S. B. Razorenov, A. B. Ytkin, and V. E. Fortov, *Shocking Wave Phenomena in Solid Media* (Yanus-K, Moscow, 1996), p. 408 (in Russian).
[15] *Shock Waves and High Strain Rate Phenomena in Metals*, edited by M. A. Meyers and L. E. Murr (Plenum, New York, 1984).
[16] J. M. Ziman, *Principles of the Theory of Solids* (Mir, Moscow, 1974) (in Russian).
[17] L. D. Landau and E. M. Lifshitz, *Electrodynamic of Solids* (Nauka, Moscow, 1982), p. 46 (in Russian).
[18] J. Jersh, F. Demming, and K. Dickmann, Appl. Phys. A: Mater. Sci. Process. **64**, 29 (1997).